NeuroImage: Clinical 13 (2017) 209–214

Contents lists available at ScienceDirect

NeuroImage: Clinical

journal homepage: www.elsevier.com/locate/ynicl

Use of T1-weighted/T2-weighted magnetic resonance ratio to elucidate changes due to amyloid β accumulation in cognitively normal subjects

Fumihiko Yasuno[a,e,*], Hiroaki Kazui[b], Naomi Morita[c], Katsufumi Kajimoto[d], Masafumi Ihara[d], Akihiko Taguchi[f], Akihide Yamamoto[e], Kiwamu Matsuoka[a], Masato Takahashi[a], Jyoji Nakagawara[c], Hidehiro Iida[e], Toshifumi Kishimoto[a], Kazuyuki Nagatsuka[d]

[a]Department of Psychiatry, Nara Medical University, Kashihara, Japan
[b]Department of Neuropsychiatry, Osaka University Medical School, Suita, Japan
[c]Department of Radiology, National Cerebral and Cardiovascular Center, Suita, Japan
[d]Department of Neurology, National Cerebral and Cardiovascular Center, Suita, Japan
[e]Department of Investigative Radiology, National Cerebral and Cardiovascular Center, Suita, Japan
[f]Department of Regenerative Medicine Research, Institute of Biomedical Research and Innovation, Kobe, Japan

ARTICLE INFO

Article history:
Received 29 July 2016
Received in revised form 25 November 2016
Accepted 26 November 2016
Available online 2 December 2016

Keywords:
Alzheimer's disease (AD)
Amyloid-β (Aβ)
^{11}C–labeled Pittsburgh Compound B ([^{11}C]PiB)
Positron emission tomography (PET)
T1-weighted/T2-weighted magnetic resonance ratio images

ABSTRACT

The ratio of signal intensity in T1-weighted (T1w) and T2-weighted (T2w) magnetic resonance imaging (MRI) was recently proposed to enhance the sensitivity of detecting changes in disease-related signal intensity. The objective of this study was to test the effectiveness of T1w/T2w image ratios as an easily accessible biomarker for amyloid beta (Aβ) accumulation. We performed the T1w/T2w analysis in cognitively normal elderly individuals. We applied [^{11}C] Pittsburgh Compound B (PiB)-PET to the same individuals, and Aβ deposition was quantified by its binding potential (PiB-BP$_{ND}$). The subjects were divided into low and high PiB-BP$_{ND}$ groups, and group differences in regional T1w/T2w values were evaluated. In the regions where we found a significant group difference, we conducted a correlation analysis between regional T1w/T2w values and PiB-BP$_{ND}$. Subjects with high global cortical PiB-BP$_{ND}$ showed a significantly higher regional T1w/T2w ratio in the frontal cortex and anterior cingulate cortex. We found a significant positive relationship between the regional T1w/T2w ratio and Aβ accumulation. Moreover, with a T1w/T2w ratio of 0.55 in the medial frontal regions, we correctly discriminated subjects with high PiB-BP$_{ND}$ from the entire subject population with a sensitivity of 84.6% and specificity of 80.0%. Our results indicate that early Aβ-induced pathological changes can be detected using the T1w/T2w ratio on MRI. We believe that the T1w/T2w ratio is a prospective stable biological marker of early Aβ accumulation in cognitively normal individuals. The availability of such an accessible marker would improve the efficiency of clinical trials focusing on the initial disease stages by reducing the number of subjects who require screening by Aβ-PET scan or lumbar puncture.

1. Introduction

The amyloid beta (Aβ) cascade is currently the most convincing hypothesis for the pathogenesis of Alzheimer's disease (AD), suggesting that the formation of senile plaques followed by the deposition of Aβ are the earliest pathological changes in the disease (Hardy and Selkoe, 2002; Hardy and Higgins, 1992). Recent evidence has shown that amyloid pathology occurs >20 years before the clinical onset of AD (Bateman et al., 2012; Jack et al., 2013). Therefore, biomarker-based detection of the initial Aβ pathology is important for better clinical management of AD, potentially providing the opportunity to start disease-modifying therapies before the progression stages of AD.

The accumulation of brain Aβ can be assessed by measurement of the Aβ concentration in the cerebrospinal fluid (CSF) or by molecular imaging techniques such as positron emission tomography (PET) using a specific radioligand for Aβ. However, lumbar puncture, needed for the collection of a CSF sample, is associated with the risk of a clinically noxious event and thus is unsuitable as a mass screening tool.

Abbreviations: Aβ, amyloid beta; AD, Alzheimer's disease; BP, binding potential; CSF, cerebrospinal fluid; FWHM, full-width at half maximum; MRI, magnetic resonance imaging; PET, positron emission tomography; PiB, Pittsburgh Compound B; PiB-BP$_{ND}$, PiB-BP estimates relative to non-displaceable (ND) binding; ROC, receiver operating characteristic; T1w, T1-weighted; T2w, T2-weighted; VOI, volumes of interest.

* Corresponding author at: Department of Psychiatry, Nara Medical University, 840 Shijocho, Kashihara, Nara 634-8522, Japan.
E-mail address: ejm86rp@yahoo.co.jp (F. Yasuno).

http://dx.doi.org/10.1016/j.nicl.2016.11.029

Neuroimaging has the merit of being less invasive. However, PET is relatively expensive, and its availability is limited. Furthermore, PET leads to cumulative radiation exposure of subjects (Tosun et al., 2014).

Magnetic resonance imaging (MRI) is an appealing candidate for the inexpensive and noninvasive identification of surrogate biomarkers for altered brain anomalies in neurological and psychiatric diseases. The ratio of the signal intensities of T1-weighted (T1w) and T2-weighted (T2w) MRI was recently proposed to enhance the sensitivity of detecting changes in signal intensity associated with diseases (Glasser and Van Essen, 2011). Signal intensity changes may be a particularly sensitive measurement, as exhibited by findings in various brain diseases (e.g., infarction and multiple sclerosis), and measuring the signal intensity ratio of T1w and T2w images has conceivable advantages over standard volume/size measurements (Iwatani et al., 2015).

Recently, improved methods have been developed that use the ratio of T1w/T2w MRI images (Ganzetti et al., 2014; Shafee et al., 2015). We hypothesized that the T1w/T2w ratio analysis may also be helpful to detect signal intensity changes due to Aβ accumulation within subjects at pre-clinical stage of AD. To test this hypothesis, we examined the effectiveness of T1w/T2w ratio imaging as an easily accessible biomarker for Aβ accumulation. We applied the T1w/T2w analysis workflow (Ganzetti et al., 2014) to structural MRI data collected in cognitively normal elderly individuals. For comparison to standard PET techniques, we performed [^{11}C] Pittsburgh Compound B (PiB)-PET in the same individuals, and Aβ deposition was quantified by cortical binding potential (PiB-BP$_{ND}$). The main purpose of this study was to develop a new method for screening patients for high accumulation of Aβ deposits by using the ratio of the signal intensities in T1w and T2w images.

2. Materials and methods

2.1. Participants

Thirty-eight cognitively normal older participants were recruited from the local area by poster advertisements. The inclusion criteria were an age of 55–85 years, a mini-mental state examination score of 27 or higher, independent living in the community, and no major structural abnormalities or signs of major vascular pathology on MRI. The exclusion criteria included major neurological, psychiatric, or medical illnesses; the use of medications that affect cognition; and MRI contraindications. This study was carried out in accordance with The Code of Ethics of the World Medical Association (Declaration of Helsinki) for experiments involving humans. The study was approved by the institutional review boards of all of the participating institutions, and all participants gave written informed consent.

2.2. PET and MRI scans

PET and MRI examination methods have been described in detail previously (Yasuno et al., 2016). PET examinations were performed with a Biograph mCT (Siemens, Knoxville Healthcare/Molecular Imaging, TN, USA). [^{11}C]PiB (645 ± 30 MBq) was intravenously injected with 50 mL of saline. A sequence of 33 scans was acquired during the 70 min (4 × 15 s, 8 × 30 s, 9 × 1 min, 2 × 3 min, and 10 × 5 min) after the [^{11}C]PiB injection. All MRI examinations were performed using a 3.0-Tesla whole-body scanner (Signa Excite HD V12M4; GE Healthcare, Milwaukee, WI, USA) with an 8-channel phased-array brain coil. High-resolution three-dimensional T1-weighted images were acquired using a spoiled gradient-recalled sequence (TR = 12.8 ms, TE = 2.6 ms, flip angle = 8°, FOV, 256 mm; 188 sections in the sagittal plane; acquisition matrix, 256 × 256; acquired resolution, 1 × 1 × 1 mm). T2-weighted images were obtained using a fast-spin echo sequence (TR = 4800 ms; TE = 101 ms; echo train length (ETL) = 8; FOV = 256 mm; 74 slices in the transverse plane; acquisition matrix, 160 × 160, acquired resolution, 1 × 1 × 2 mm).

Table 1
Demographic statistics of low and high PiB-BP$_{ND}$ groups.

Characteristic/test	Low PiB-BP$_{ND}$ (BP < 0.20)	High PiB-BP$_{ND}$ (BP ≥ 0.20)	t or χ^2	p
No.	25	13		
Global cortical mean PiB-BP$_{ND}$	0.10 ± 0.07	0.40 ± 0.26	4.06	0.001[a]
Age, years	70.2 ± 6.9	70.8 ± 7.0	0.24	0.810
Sex M/F	19/6	4/9	7.32	0.007[a]
Education, years	14.4 ± 2.5	11.7 ± 2.3	3.27	0.002[a]
Mini-mental state examination	29.3 ± 0.9	29.5 ± 1.1	0.54	0.590

Data are represented as mean ± sd.
[a] p < 0.05.

Table 2
Differences in regional T1w/T2w ratio between low and high PiB-BP$_{ND}$ groups.

Regions	T1w/T2w ratio		t-Test[a]	
	Low PiB-BP$_{ND}$ (N = 25) (BP < 0.20)	High PiB-BP$_{ND}$ (N = 13) (BP ≥ 0.20)	t (1, 31)	p
Orbital frontal cortex	0.78 ± 0.06	0.84 ± 0.08	2.54	0.02[b]
Lateral prefrontal cortex	0.70 ± 0.06	0.74 ± 0.05	2.10	0.04[b]
Medial prefrontal cortex	0.64 ± 0.05	0.68 ± 0.04	2.63	0.01[b]
Lateral temporal cortex	0.76 ± 0.05	0.79 ± 0.04	1.69	0.10
Medial temporal cortex	0.70 ± 0.05	0.73 ± 0.03	1.72	0.09
Parietal cortex	0.71 ± 0.05	0.70 ± 0.06	0.05	0.96
Occipital cortex	0.76 ± 0.06	0.77 ± 0.05	0.50	0.62
Striatum	0.90 ± 0.06	0.93 ± 0.05	1.38	0.18
Anterior cingulate cortex	0.63 ± 0.04	0.66 ± 0.04	2.48	0.02[b]
Posterior cingulate cortex	0.69 ± 0.04	0.72 ± 0.05	1.96	0.06

[a] Repeated measures of analysis of variance revealed a significant interaction of regions × groups of low/high PiB-BP$_{ND}$ (regions, F = 235.4, df = 3.6, 128.2, p < 0.01, regions × groups of low/high PiB-BP$_{ND}$; F = 2.54, df = 3.6, 128.2, p = 0.05, groups of low/high PiB-BP$_{ND}$; F = 3.87, df = 1, 36, p = 0.06).
[b] p < 0.05.

2.3. PET data analysis

PET data analysis has been previously described in detail (Yasuno et al., 2016). [^{11}C]PiB-PET data were corrected for partial volume effects using an algorithm introduced by Muller-Gartner et al. (1992) that was implemented in the PMOD software package (PMOD V.3.3; PMOD Technologies GmbH, Adliswil, Switzerland). The radioactivity levels in six brain regions (the prefrontal cortex, lateral temporal cortex, parietal cortex, anterior cingulate cortex, posterior cingulate cortex, and cerebellum) were obtained with a template-based method for defining volumes of interest (VOI) (Yasuno et al., 2002). Regional time-activity data were analyzed from 35 to 70 min of PET data with the Logan graphical method (Logan et al., 1996). This method yields BP estimates relative to non-displaceable (ND) binding, which is denoted by BP$_{ND}$ (Innis et al., 2007). Global cortical mean PiB-BP$_{ND}$ was evaluated from the measured brain regions.

2.4. MRI data analysis of T1w/T2w images

T1w and T2w images were preprocessed and combined using a dedicated workflow as described in the previous papers by Ganzetti et al. (2014, 2015). This includes bias correction and intensity calibration on

Table 3
Correlation between T1w/T2w ratio and PiB-BP$_{ND}$ in measured regions.

	Spearman's ρ (p)
Orbital frontal cortex	0.21 (0.21)
Lateral prefrontal cortex	0.24 (0.14)
Medial prefrontal cortex	0.54 (0.0005)[a]
Anterior cingulate cortex	0.25 (0.13)
Combination of the above regions	0.45 (0.005)[a]

[a] Significant with consideration to the multiple comparisons with p < 0.01 (0.05/5).

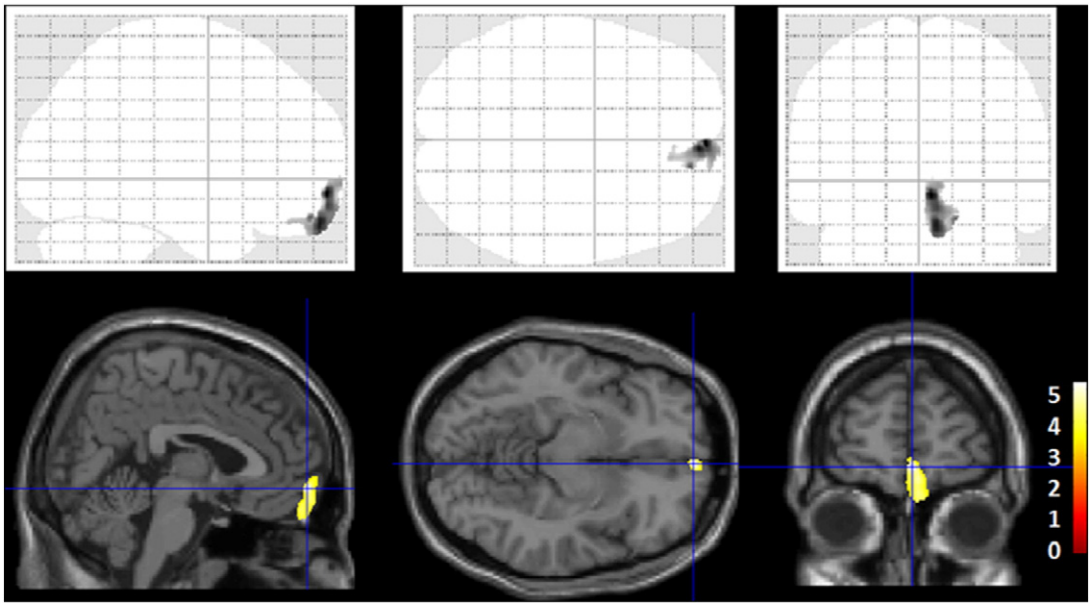

Fig. 1. Images of voxel-based maps showing greater T1w/T2w ratios in the region of the medial frontal cortex in the high PiB-BP_{ND} group compared to the low PiB-BP_{ND} group. $p < 0.001$, uncorrected. The statistical parametric mapping projections were superimposed on representative sagittal ($x = 4$), transaxial ($z = -8$) and coronal ($y = 60$) magnetic resonance images.

each of the two images and the subsequent calculation of the ratio between preprocessed T1w and T2w images. The entire processing of the T1w/T2w image was conducted using the MR Tool–Multimodal Mapping (http://www.bindgroup.eu/wp-content/uploads/2015/11/mrtool-v1.2.zip) implemented in the SPM12 software (Wellcome Trust Centre for Neuroimaging, London, UK).

Initially, the original T2w image was coregistered to the T1w image through a rigid-body transformation. Then, the T1w and T2w images were separately subjected to bias correction. The input parameters for the bias correction algorithm, namely the smoothing and the regularization parameters, were set at their default value. After correcting for intensity non-uniformity, the T1w and T2w images were further processed to standardize their intensity by using a linear scaling procedure systematically described in Ganzetti et al. (2014, 2015). Eventually, after calibrating the T1w and T2w images, their ratio was calculated to generate the calibrated T1w/T2w image. To conduct statistical comparisons between groups, we spatially transformed the T1w/T2w image in subject space to the Montreal Neurological Institute space. The gray matter (GM) and white matter (WM) components of the T1w/T2w image were extracted using the segmented normalized T1w image. We created both GM and WM binary mask images using the SPM Masking Toolbox (Ridgway et al., 2009). These mask images were used to perform the statistical analyses with SPM12.

2.5. Statistical analysis

The subjects were divided into low and high PiB-BP_{ND} groups according to the global cortical mean PiB-BP_{ND}. We regarded subjects with PiB-BP_{ND} <0.20 as the low PiB-BP_{ND} group ($n = 25$) and those with PiB-BP_{ND} ≥0.20 as the high PiB-BP_{ND} group ($n = 13$). Group differences in demographic characteristics between the low and high PiB-BP_{ND} groups were examined by unpaired *t*-test and Pearson's χ^2 test.

Group differences in regional T1w/T2w values were compared using repeated measures analysis of variance (ANOVA) with a Huynh-Feldt's correction. A follow-up *t*-test was performed on the T1w/T2w values of each measured region in the two PiB-BP_{ND} groups. Although we found significant differences in sex and education between the groups, we did not include these as covariates due to the lack of a significant linear relationship with regional PiB-BP_{ND}. In the regions where we found a significant difference of T1w/T2w values between groups, we conducted a correlation analysis between the regional T1w/T2w values and PiB-BP_{ND} by Spearman correlation tests.

Voxel-based analysis was performed using the SPM12 software. Both GM and WM T1w/T2w images were smoothed with a Gaussian kernel of 6-mm full-width at half-maximum (FWHM). The difference in GM and WM T1w/T2w values between groups of low and high PiB-BP_{ND} was examined using ANOVA. Multiple comparisons were controlled with cluster-extent threshold combined with a height threshold of 0.001, to produce clusters with a family-wise error of $p < 0.05$. Spherical VOIs (5-mm radius) were determined from regions in which subjects with high PiB-BP_{ND} showed significantly higher or lower T1w/T2w values than subjects with low PiB-BP_{ND}. The center of the spherical VOIs was determined from the Montreal Neurological Institute coordinates with peak *t*-value. The regional T1w/T2w values were calculated by averaging the values for all voxels within the spherical VOIs placed on T1w/T2w images. The differences of T1w/T2w values in spherical VOIs were examined by unpaired *t*-test. The relationships among T1w/T2w values, PiB-BP_{ND} in the spherical VOIs, and global cortical mean PiB-BP_{ND} were examined by Spearman correlation tests. Statistical tests were 2-tailed and significance was reported at $\alpha < 0.05$. Statistical analysis of the data was performed using SPSS for Windows 22.0 (IBM Japan Inc., Tokyo, Japan).

3. Results

Table 1 summarizes the demographic and clinical characteristics of groups of low and high global cortical mean PiB-BP_{ND}. The groups differ significantly in sex and educational periods.

In the repeated measures ANOVA, we found significant interaction between measured regions and the low/high groups of PiB-BP_{ND} (Table 2), and the follow-up *t*-test indicated that subjects with high global cortical PiB-BP_{ND} showed significantly higher regional T1w/T2w ratio in the orbital frontal cortex, lateral prefrontal cortex, medial frontal cortex, and anterior cingulate cortex (Table 2). Although we found significant differences in sex and education between groups, we did not include them as covariates due to the lack of their significant linear relationship with regional PiB-BP_{ND}.

In the correlation analysis between the regional T1w/T2w ratio and PiB-BP_{ND}, we found a significant correlation between these values in the medial frontal cortex and in the combined region analysis (Table 3).

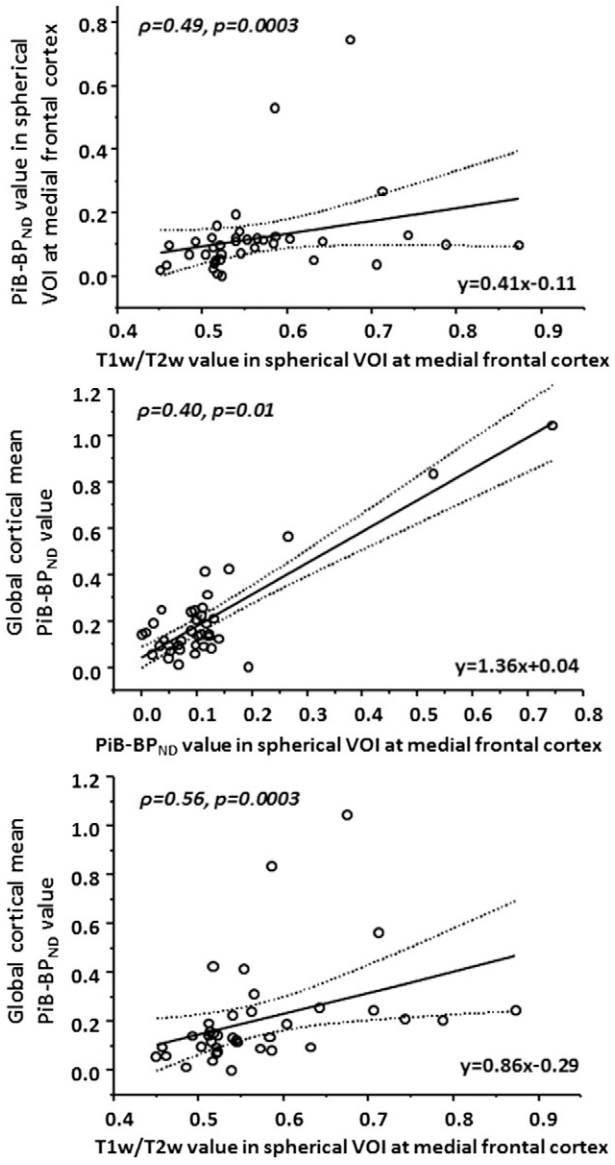

Fig. 2. Scatter plots of the relationships among the T1w/T2w ratios, regional PiB-BP$_{ND}$ values, and the global cortical mean PiB-BP$_{ND}$ values. We found significant positive correlations among the regional T1w/T2w ratios, regional PiB-BP$_{ND}$ values, and global cortical mean PiB-BP$_{ND}$ values. Fitted lines (solid) with 95% confidence intervals (dashed lines) are shown in each plot. $p < 0.05$; ρ, Spearman's ρ; VOI, volume of interest.

In the voxel-based analysis, patients with high PiB-BP$_{ND}$ values showed significantly higher GM T1w/T2w ratios in the medial frontal region ($x = 4, y = 60, z = -8$) than patients with low PiB-BP$_{ND}$ values (0.53 ± 0.04 in the low, 0.65 ± 0.11 in the high PiB-BP$_{ND}$ group in the spherical VOI, $t = 3.93$, $p = 0.001$) (Fig. 1). We found no significant difference in WM T1w/T2w ratios between groups. After correcting the bias and calibrating the intensity, we compared GM T1w and T2w images in the medial frontal region between groups and found that T2w images in the high PiB-BP$_{ND}$ group had significantly lower intensity (31.1 ± 2.6 in the low, 30.6 ± 2.6 in the high PiB-BP$_{ND}$ group, $t = 0.62$, $p = 0.54$ for T1w images; 50.5 ± 4.3 in the low, 44.7 ± 5.8 in the high PiB-BP$_{ND}$ group, $t = 3.48$, $p = 0.001$ for T2w images).

Scatter plots of the relationships among the T1w/T2w ratio and PiB-BP$_{ND}$ in the spherical VOI in the medial prefrontal region and the global cortical mean PiB-BP$_{ND}$ are shown in Fig. 2. We found significant correlations among regional T1w/T2w ratios, regional PiB-BP$_{ND}$ values, and global cortical mean PiB-BP$_{ND}$ values.

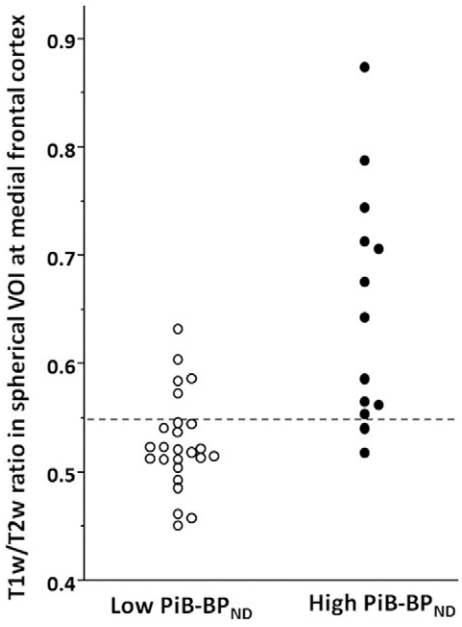

Fig. 3. Scatter plot of the T1w/T2w ratios in the medial frontal region of the low and high PiB-BP$_{ND}$ groups. With a T1w/T2w ratio of 0.55, we correctly predicted 11 of 13 high PiB-BP$_{ND}$ group members and 20 of 25 low PiB-BP$_{ND}$ group members.

Fig. 3 shows the scatter plot of T1w/T2w ratio in the medial frontal region of the low and high PiB-BP$_{ND}$ groups. We found a significant difference in the T1w/T2w ratios between the groups. We performed receiver operating characteristic curve (ROC) analysis to find the cut-off point of the T1w/T2w ratio that maximized sensitivity or specificity, which could best differentiate patients with low PiB-BP$_{ND}$ from high PiB-BP$_{ND}$ group members (Fig. 4). With a T1w/T2w ratio of 0.55, we correctly predicted 11 of 13 high PiB-BP$_{ND}$ group members and 20 of 25 low PiB-BP$_{ND}$ group members. The accuracy was 81.6%, with a sensitivity of 84.6% and specificity of 80.0% for the discrimination of subjects with high PiB-BP$_{ND}$ from the total pool of subjects.

4. Discussion

In this present study, we evaluated the potential utility of the T1w/T2w approach for the prediction of Aβ deposition by the analysis of

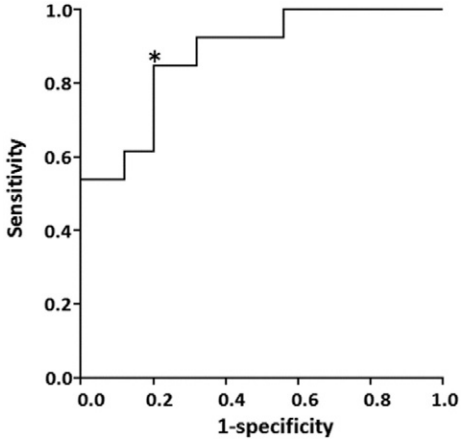

Fig. 4. Receiver operating characteristic curve for the T1w/T2w ratio. With the T1w/T2w ratio of 0.55, Youden index [sensitivity − (1-specificity)] shows a maximum value of 0.65 (sensitivity = 0.846, specificity = 0.800) at the cutpoint shown by asterisk.

T1w and T2w data collected in cognitively normal subjects with low and high cortical Aβ accumulation. To our knowledge, this is the first in vivo study to show a relationship between the T1w/T2w ratio and amyloid pathology. We found larger T1w/T2w ratios in the high PiB-BP_{ND} group and a significant positive correlation between the T1w/T2w ratios and PiB-BP_{ND} values.

Our results support the notion that the ratio of T1w/T2w images could be a potentially sensitive marker of amyloid accumulation at the pre-clinical stage. However, the positive relationship between T1w/T2w ratio and the amyloid accumulation was contrary to expectations. If the T1w/T2w ratio were a reflection of the myelin-related pathological changes due to toxic Aβ accumulation, the T1w/T2w ratio should be decreased in accordance with the increase in Aβ accumulation. To interpret our results, it should be considered that the T1w/T2w image may reflect not only the level of demyelination but also other microstructural factors in addition to myelin. For example, iron, in addition to myelin, has been found to contribute to cortical MR image contrast (Shafee et al., 2015). Indeed, most metal deposition, including iron, causes high signal intensity on T1w images and/or low signal intensity on T2w images (Kanda et al., 2016). In the present study, we found that T2w images in the high PiB-BP_{ND} group had a significantly lower intensity compared to the low PiB-BP_{ND} group, and the increased T1w/T2w ratio is primarily due to differences in the T2w image.

Under normal conditions in healthy subjects, iron and myelin are colocalized in the cortex (Fukunaga et al., 2010), and the large fraction of the differences in T1w/T2w is thought to be due to variation of the myelin density (Shafee et al., 2015). However, recent reports provide strong evidence regarding the covariance of Aβ plaques with the heme-rich deposits found in the regions of the brain consistent with the pathological profile of neurodegeneration in AD (Raha et al., 2013). Iron complexed with Aβ peptides was indicated to be toxic in cultured cells (Schubert and Chevion, 1995). Iron was also shown to initiate and promote the aggregation, oligomerization, and amyloidosis of Aβ peptides (Huang et al., 2004; Liu et al., 2011; Mantyh et al., 1993). Thus, our finding of a positive relationship between the T1w/T2w ratio and Aβ deposition may reflect perturbations in the magnetic field due to plaque-attached iron strong enough to affect tissue susceptibility and MR relaxation times.

In vivo detection of amyloid plaques in humans by MRI opens up the possibility of the promising scenario of AD prevention. Here, we showed that the T1w/T2w ratio in the medial frontal cortex could classify 80.0% of subjects with low PiB-BP_{ND} and 84.6% of subjects with high PiB-BP_{ND}, with an accuracy of 81.6%. We believe that the T1w/T2w ratio is a potential stable biological marker of the early Aβ accumulation in cognitively normal individuals. As such, the T1w/T2w ratio method may aid the recruitment of subjects and the evaluation of the therapeutic efficacy in clinical settings and trials. Such a method of classifying Aβ-positivity improves the efficiency of the clinical trials by reducing subjects who need to be screened by CSF analysis or Aβ-PET. Our method is also useful for the identification of individuals with Aβ+ deposits in the situation in which cost or a logistic problem prohibits Aβ detection by Aβ-PET scan or lumbar puncture.

The limitations of our study need to be considered. First, the sample size of our study was not large enough to detect small differences between the groups. Second, this was a cross-sectional and not a longitudinal follow-up study, which is necessary to see how predictive our findings are of future AD. Third, when we focused on three outliers with high regional T1w/T2w values in Fig. 2, these values seem to be overestimated when compared to those predicted from their PiB-BP_{ND} in plots without these outliers. This overestimation might be due to other confounding factors that affect the T1w/T2w values besides the known iron and myelin-related pathological changes. Before the clinical application of the T1w/T2w ratio method, future studies should determine the possible factors other than the iron and myelin content that affect the T1w/T2w ratio in MRI.

5. Conclusions

Our results showed that early Aβ deposits can be detected using the T1w/T2w ratio in MRI. We found a significant positive relationship between the regional T1w/T2w ratio and Aβ accumulation. This method is an attractive candidate for an inexpensive and noninvasive surrogate biomarker of Aβ accumulation because it is available widely and is routinely evaluated in clinical practice. The relatively short scan times and conventional protocols also increase the utility of this method in the clinical situation. Whereas it would be premature to draw definitive conclusions from the current analysis, our findings serve as promising pilot data for future studies.

Conflict of interests

All authors declare that there are no competing interests.

Funding

This research was supported by Grants-in-Aid for Scientific Research (C) 15K09841 from the Japan Society for the Promotion of Science. The funding body had no role in this study or its publication.

Acknowledgements

We thank Yuko Yamamoto in the Department of Neuropsychiatry at Osaka University Medical School for the recruitment and care of participants. We thank Akihide Shimizu, Yusuke Terakawa, Keiji Matsumuro, and the members of the PET staff of the Department of Radiology at the National Cerebral and Cardiovascular Center for carrying out the acquisition of PET data.

References

Bateman, R.J., Xiong, C., Benzinger, T.L., Fagan, A.M., Goate, A., Fox, N.C., Marcus, D.S., Cairns, N.J., Xie, X., Blazey, T.M., Holtzman, D.M., Santacruz, A., Buckles, V., Oliver, A., Moulder, K., Aisen, P.S., Ghetti, B., Klunk, W.E., McDade, E., Martins, R.N., Masters, C.L., Mayeux, R., Ringman, J.M., Rossor, M.N., Schofield, P.R., Sperling, R.A., Salloway, S., Morris, J.C., 2012. Clinical and biomarker changes in dominantly inherited Alzheimer's disease. N. Engl. J. Med. 367, 795–804.

Fukunaga, M., Li, T.Q., van Gelderen, P., de Zwart, J.A., Shmueli, K., Yao, B., Lee, J., Maric, D., Aronova, M.A., Zhang, G., Leapman, R.D., Schenck, J.F., Merkle, H., Duyn, J.H., 2010. Layer-specific variation of iron content in cerebral cortex as a source of MRI contrast. Proc. Natl. Acad. Sci. U. S. A. 107, 3834–3839.

Ganzetti, M., Wenderoth, N., Mantini, D., 2014. Whole brain myelin mapping using T1- and T2-weighted MR imaging data. Front. Hum. Neurosci. 8, 671.

Ganzetti, M., Wenderoth, N., Mantini, D., 2015. Mapping pathological changes in brain structure by combining T1- and T2-weighted MR imaging data. Neuroradiology 57, 917–928.

Glasser, M.F., Van Essen, D.C., 2011. Mapping human cortical areas in vivo based on myelin content as revealed by T1- and T2-weighted MRI. J. Neurosci. 31, 11597–11616.

Hardy, J.A., Higgins, G.A., 1992. Alzheimer's disease: the amyloid cascade hypothesis. Science 256, 184–185.

Hardy, J., Selkoe, D.J., 2002. The amyloid hypothesis of Alzheimer's disease: progress and problems on the road to therapeutics. Science 297, 353–356.

Huang, X., Atwood, C.S., Moir, R.D., Hartshorn, M.A., Tanzi, R.E., Bush, A.I., 2004. Trace metal contamination initiates the apparent auto-aggregation, amyloidosis, and oligomerization of Alzheimer's Abeta peptides. J. Biol. Inorg. Chem. 9, 954–960.

Innis, R.B., Cunningham, V.J., Delforge, J., Fujita, M., Gjedde, A., Gunn, R.N., Holden, J., Houle, S., Huang, S.C., Ichise, M., Iida, H., Ito, H., Kimura, Y., Koeppe, R.A., Knudsen, G.M., Knuuti, J., Lammertsma, A.A., Laruelle, M., Logan, J., Maguire, R.P., Mintun, M.A., Morris, E.D., Parsey, R., Price, J.C., Slifstein, M., Sossi, V., Suhara, T., Votaw, J.R., Wong, D.F., Carson, R.E., 2007. Consensus nomenclature for in vivo imaging of reversibly binding radioligands. J. Cereb. Blood Flow Metab. 27, 1533–1539.

Iwatani, J., Ishida, T., Donishi, T., Ukai, S., Shinosaki, K., Terada, M., Kaneoke, Y., 2015. Use of T1-weighted/T2-weighted magnetic resonance ratio images to elucidate changes in the schizophrenic brain. Brain Behav. 5, e00399.

Jack Jr., C.R., Knopman, D.S., Jagust, W.J., Petersen, R.C., Weiner, M.W., Aisen, P.S., Shaw, L.M., Vemuri, P., Wiste, H.J., Weigand, S.D., Lesnick, T.G., Pankratz, V.S., Donohue, M.C., Trojanowski, J.Q., 2013. Tracking pathophysiological processes in Alzheimer's disease: an updated hypothetical model of dynamic biomarkers. Lancet Neurol. 12, 207–216.

Kanda, T., Nakai, Y., Aoki, S., Oba, H., Toyoda, K., Kitajima, K., Furui, S., 2016. Contribution of metals to brain MR signal intensity: review articles. Jpn. J. Radiol. 34, 258–266.

Liu, B., Moloney, A., Meehan, S., Morris, K., Thomas, S.E., Serpell, L.C., Hider, R., Marciniak, S.J., Lomas, D.A., Crowther, D.C., 2011. Iron promotes the toxicity of amyloid beta peptide by impeding its ordered aggregation. J. Biol. Chem. 286, 4248–4256.

Logan, J., Fowler, J.S., Volkow, N.D., Wang, G.J., Ding, Y.S., Alexoff, D.L., 1996. Distribution volume ratios without blood sampling from graphical analysis of PET data. J. Cereb. Blood Flow Metab. 16, 834–840.

Mantyh, P.W., Ghilardi, J.R., Rogers, S., DeMaster, E., Allen, C.J., Stimson, E.R., Maggio, J.E., 1993. Aluminum, iron, and zinc ions promote aggregation of physiological concentrations of beta-amyloid peptide. J. Neurochem. 61, 1171–1174.

Muller-Gartner, H.W., Links, J.M., Prince, J.L., Bryan, R.N., McVeigh, E., Leal, J.P., Davatzikos, C., Frost, J.J., 1992. Measurement of radiotracer concentration in brain gray matter using positron emission tomography: MRI-based correction for partial volume effects. J. Cereb. Blood Flow Metab. 12, 571–583.

Raha, A.A., Vaishnav, R.A., Friedland, R.P., Bomford, A., Raha-Chowdhury, R., 2013. The systemic iron-regulatory proteins hepcidin and ferroportin are reduced in the brain in Alzheimer's disease. Acta Neuropathol. Commun. 1, 55.

Ridgway, G.R., Omar, R., Ourselin, S., Hill, D.L., Warren, J.D., Fox, N.C., 2009. Issues with threshold masking in voxel-based morphometry of atrophied brains. NeuroImage 44, 99–111.

Schubert, D., Chevion, M., 1995. The role of iron in beta amyloid toxicity. Biochem. Biophys. Res. Commun. 216, 702–707.

Shafee, R., Buckner, R.L., Fischl, B., 2015. Gray matter myelination of 1555 human brains using partial volume corrected MRI images. NeuroImage 105, 473–485.

Tosun, D., Joshi, S., Weiner, M.W., 2014. Multimodal MRI-based imputation of the Abeta+ in early mild cognitive impairment. Ann. Clin. Transl. Neurol. 1, 160–170.

Yasuno, F., Hasnine, A.H., Suhara, T., Ichimiya, T., Sudo, Y., Inoue, M., Takano, A., Ou, T., Ando, T., Toyama, H., 2002. Template-based method for multiple volumes of interest of human brain PET images. NeuroImage 16, 577–586.

Yasuno, F., Kazui, H., Morita, N., Kajimoto, K., Ihara, M., Taguchi, A., Yamamoto, A., Matsuoka, K., Kosaka, J., Kudo, T., Iida, H., Kishimoto, T., Nagatsuka, K., 2016. High amyloid-beta deposition related to depressive symptoms in older individuals with normal cognition: a pilot study. Int. J. Geriatr. Psychiatry 31, 920–928.